Wormhole-Like Mesoporous Carbons from Gelatine as Multistep Infiltration Effect

Maria Ulfa[1,2,*], Wega Trisunaryanti[2], Iip Izul Falah[2], and Indriana Kartini[2]

[1]*Chemical Education Study Program, Faculty of Teacher Training and Education, Sebelas Maret University, Jl. Ir. Sutami 36A, Surakarta 57126, Central Java Indonesia*

[2]*Department of Chemistry, Faculty of Mathematics and Natural Sciences, Universitas Gadjah Mada, Sekip Utara PO BOX BLS 21 Yogyakarta 55281, Indonesia*

ABSTRACT

Wormhole-like mesoporous carbon from gelatine (WMCG) with two different pore diameters have been synthesized by adopting a modified infiltration treatment. The infiltration effect on the morphology was investigated. The results show that the WMCG sample was obtained after dehydration, pyrolysis and silica removal process. The pore diameters WMCG are 15.2 and 4.8 nm with specific surface areas of 280 m^2/g, total pore volumes of 0.5 cm^3/g and the thermal stability up to 1400 °C. The bimodal pore of WMCG obtained as the high step of infiltration level effect.

Keywords: *gelatine; infiltration; wormhole-like mesoporous carbon*

ABSTRAK

Karbon mesopori dari gelatine mirip lubang cacing (WMCG) dengan dua diameter pori yang berbeda telah disintesis dengan mangambil perlakukan infiltrasi termodifikasi. Efek infiltrasi pada morfologi telah diinvestigasi. Hasil menunjukkan bahwa sampel WMCG didapatkan setelah proses dehidrasi, pirolisis dan pelepasan silika. Diameter pori WMCG berturut-turut adalah 15,2 dan 4,8 nm dengan luas permukaan spesifik adalah 280 m^2/g, volume pori total 0.5 cm^3/g dan kestrabilan termal 1400 °C. Pori ganda WMCG berasal dari efek level infiltrasi tahap tinggi.

Kata Kunci: *gelatin; infiltrasi; karbon mesopori mirip lubang cacing*

INTRODUCTION

The wormhole-like mesoporous carbon (WMC) with bimodal pore is interesting type of carbon due to its three dimensional morphology with high surface area. The previous research of synthesized wormhole-like carbon using soft template. The hard template research to get mesoporous carbon-using gelatine as precursor carbon to get wormhole-like mesoporous carbon has never been reported before.

In our previous paper, the honeycomb like as regular pore MCGe was successfully synthesized by using hard template method using gelatine as precursor to create pore on carbon and SBA-15 at low loading of precursor but just get a little carbon [1-3]. In order to get more carbon, we try to increase loading of precursor. The infiltration gelatine into SBA-15 pores via hydrogen bonding between silicate species and amine group (Fig. 1). However, the high loading of precursor might be one factor on destruction of material morphology due to the uncompleted pore filling process at least to produce lot of carbon [4-5].

The infiltration precursor into hard template must be conducted by special treatment in order to get more carbon without disordered the uniformity of material. So, based on the consideration above, the authors performed synthesis and characterization of wormhole-like mesoporous carbon using the hard template method with various infiltration treatments in high precursor loading in order to get some new information about the effect of those treatments on the morphology of WMCG.

EXPERIMENTAL SECTION

Materials

SBA-15 (Commercial grade), gelatine (result of extraction at previous work) [1-3], sulfuric acid solution (66%), HF, distillated water (Merck).

Instrumentation

Nitrogen adsorption/desorption was performed on a Quantachrome Autosorb Automated Gas Sorption

---

* Corresponding author.
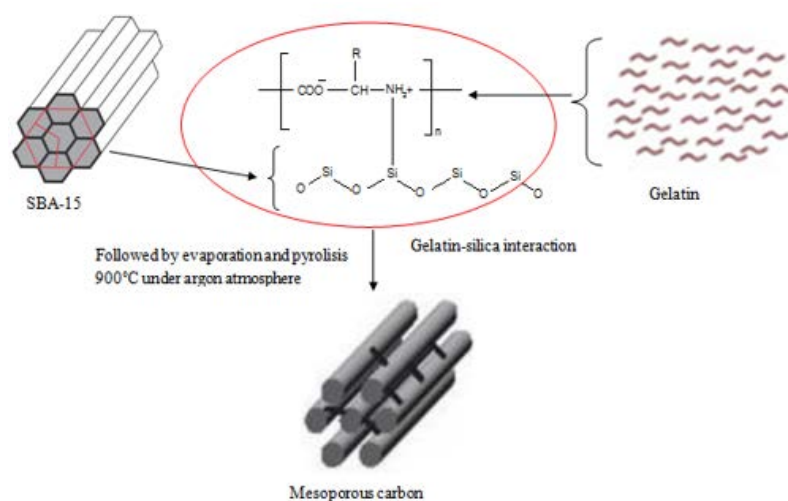Email address : ulfa.maria2015@gmail.com

Fig 1. The illustration of gelatin-silica interaction during synthesis of ideal mesoporous carbon

System, with an outgas temperature of 200 °C and a bath temperature of 77 K. Analysis of the N_2 adsorption data was performed at Autosorb 1® for windows 1.2 provided by Quantachrome Co. The surface area was calculated through a multipoint BET model using the P/P_0 ranging from 0.05 to 0.2. The PSD was calculated using a BJH model; and the total pore size was calculated in terms of the maximum P/P_0 point. The primary mesopore volume V_p, the micropore volume V_{mi}, and the external surface area S_{ext} were obtained using the high-resolution α_s-plot method [17-20]. Li-Chrospher Si-1000 silica gel (S_{BET} 25 m^2/g) and a nonporous carbon black Cabot 280 was used as a reference adsorbent.

Transition Electron Microscopy (TEM) images were obtained on a JEOL 2011, and Scanning Electron Microscope equipped with EDAX (Genesis) Energy Dispersive X-ray (EDX) system permits submicrometer elemental identification and compositional analysis. Energy Dispersive X-ray sample was prepared by depositing particles in alcohol suspension on carbon-covered nickel grids.

Thermogravimetric (TGA) measurements were carried out using a Netzsch derivatograph STA 449 F1 Jupiter (Netzsch, Germany) in the range from 40 to 1400 °C at a heating rate of 5 °C·min^{-1}. The measurements were carried out in an open Al_2O_3 crucible under helium or a synthetic air atmosphere at a flow rate of 40 mL·min^{-1}. An empty, open crucible was used as a reference.

Procedure

Synthesis of wormhole-like mesoporous carbon of gelatine (WMCG)

The mesoporous silica (SBA-15) as a template was reacted with the gelatine in a sulfuric acid solution at ratio gelatine to acid and SBA-15 (2:8:1(b/w)). The gelatine-SBA-15 composite was then pyrolyzed under argon flow at 900 °C for 3 h to carbonize the polymer and finished by silica removal from the composite using NaOH solution at temperature of 90 °C. The sample denoted as WMCG-x, with x represent as various infiltration occurred at two (WMCG-1), three (WMCG-2) and four (WMCG-3) step.

RESULT AND DISCUSSION

Fig. 1 showed an illustration of silicate-gelatine interaction. When gelatine solutions are acidified, the decreasing viscosity of the amine species takes place, leading the smooth infiltration. At acidic pH, silicate species bear a negative charge large enough to efficiently interact with gelatine chains and form a precipitated composite [6-8]. In high infiltration process, growth can proceed further larger carbon particles are formed whose self-aggregation is prevented by the presence of the gelatine chains. The final size of carbon-silica composite was determined by the amount of gelatine in silica pore i.e. larger diameter was obtained for higher infiltration level whereas the packing of this gelatine is controlled by the gelatine chains organization during infiltration. The illustration show that the sorption capacities of the mesoporous silica at infiltration level 1 did not significantly different from those of infiltration level 2 or level 3 confirm by nitrogen adsorption-desorption analysis.

The isotherm of nitrogen adsorption-desorption (Fig. 2) shows the mesoporous character with hysteresis in P/P_0 0.4 and this is consistent with bimodal profile of PSD with two different pore diameters in mesoporous range (Fig. 3). The isotherm of nitrogen adsorption-desorption show typical type-IV
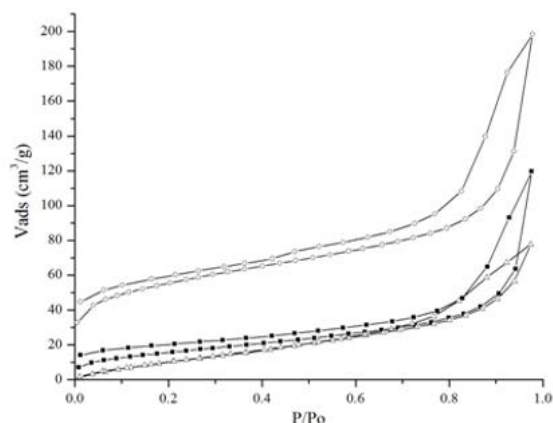
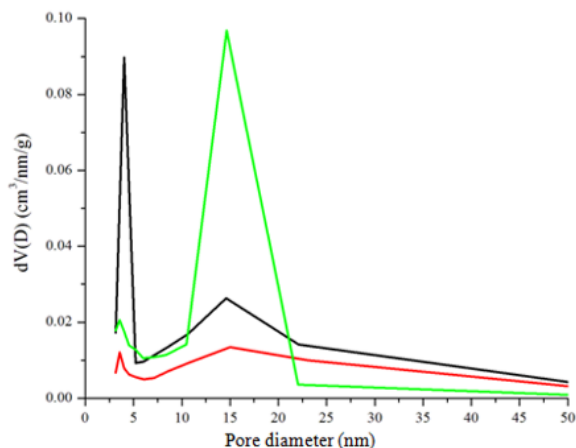**Fig 2.** Isotherm adsorption desorption of WMCG-1 (Black cube), WMCG-2 (dot white) and WMCG-3 (triangle black)

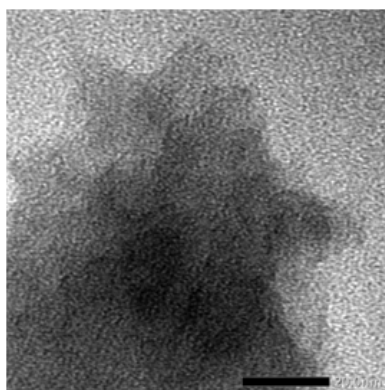**Fig 3.** The PSD profile of WMCG-1 (Black) WMCG-2 (Green) and WMCG-3(Red)

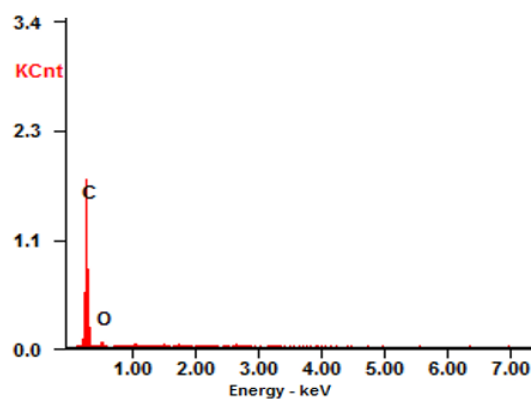**Fig 4.** TEM Images of WMCG-2 (magnification of 20 nm)

Fig 5. EDAX Profile of WMCG-2

Table 1. Textural properties of samples

Sample	I	SA (m^2/g)	PSD (nm)	Vt (cm^3/g)
WMCG-1	1	220	4.3 and 15.0	0.3
WMCG-2	2	280	4.8 and 15.2	0.5
WMCG-3	3	143	4.2 and 15.1	0.1

Note: I = Infiltration step; SA = surface area, PSD = pore size distribution; Vt = total pore volume

curves as defined by IUPAC. It is interesting that it can be found that when the infiltration level varied, the hysteresis loops of WMCG are obviously different. When the infiltration level is 1 and 3, the hysteresis loops are H1 type at about relative pressure (P/P$_0$) between 0.4 and 0.7, which implied small mesopore of the samples with an ink-bottle or cakelike type pore, i.e., to the pores with the narrower orifice and the broader inner part [9]. But when the infiltration level is 2, the hysteresis loops are H2 type at about relative pressure (P/P$_0$) between 0.7 and 0.9, which is typical of mesoporous solids consisting of very large mesopores with a large hysteresis indicating an interconnected cylinder pore system [8]. Accordingly, the pore size distribution centralized at 15.2 nm and 4.8 nm (Fig. 3). Pore

volumes of WMCG-2 are larger than that of WMCG-1 or WMCG-3, and total volumes of WMCG-1, WMCG-2 and WMCG-3 are 0.3; 0.5 and 0.1 cm^3/g, respectively (as shown in Table 1). Table 1 shows that the surface area, PSD and total pore volume increase with increasing the infiltration level. However, we found that the infiltration at three step decrease the textural properties due to the blocking pore as the high competition between acid, gelatine and water.

Fig. 4 shows the typical TEM images of WMCG-2 samples, it can be obviously visible that the microstructure of the obtained samples is disordered, which can be attributed to the strong effect of infiltration to the rapid process of filling pore. The pore type cannot be directly observed maybe because of the

wormhole-like pore structure of samples. The TEM image of WMCG (Fig. 4) shows uniform wormlike channels arranged in random fashion and distributed homogeneously throughout the bulk phase. Unlike materials with 2D-hexagonal symmetries, WMCG type materials generally possess a 3D wormhole porous framework with poorly defined crystallographic symmetry [10-13]. This perform are expected to enhance the diffusion rate of reacting species and does not require any specific orientation for the design of filtration layers.

Fig. 5 is the results of EDAX on WMCG (lower magnification, 0.5 µm) which is illustrate that the composition of samples. It is well known that the EDX technique can provide the effective atomic concentration of different substrates of investigated solids, which are present on their top surface layers [14-15]. From EDAX profile we can found that the carbon content of WMCG up to 85% represent the success conversion process during infiltration and pyrolysis. The thermogravimetric results of the WMCG materials (not shown) were performed in helium atmosphere. In these conditions, decomposition occurs without oxidation, and, consequently, weight decrease of the samples is slow. Thus, a relatively low mass loss is observed. Residual masses in this analysis had quite high values of 73-83%. The decomposition of WMCG-2 sample is very fast, and the mass loss is at 10% between 100 and 450 °C. The most intensive thermal destruction is from 700 to 1200 °C for WMCG-2 sample and the mass loss is at 8%. The stable product is observed at 1200–1400 °C and the mass total loss is 18% between 100–1400 °C. The influence of heteroatoms such as N on gelatine as carbon precursors on thermal properties could be observed in the case of these samples. So we can conclude that the amine on gelatine on this work play important role to improve the thermal stability of WMCG.

CONCLUSION

Wormhole-like mesoporous carbon of gelatine (WMCG) has been synthesized by adopting a modified infiltration treatment. The high textural properties as infiltration effect on the morphology were investigated. The results show that the WMCG have pore diameters 15.2 and 4.4 nm respectively with specific surface area of 280 m^2/g, total pore volumes of 0.5 cm^3/g and the thermal stability up to 1400 °C. The bimodal pore of WMCG obtained as the high step of infiltration level effect.

ACKNOWLEDGEMENT

REFERENCES

1. Ulfa, M., Trisunaryanti, W., Falah, I.I., Kartini, I., and Sutarno, 2014, *J. Appl. Chem.*, 7 (5), 1–7.
2. Ulfa, M., Trisunaryanti, W., Falah, I.I., Kartini, I., and Sutarno, 2014, *J. Chem. Eng.*, 4, 112–119.
3. Ulfa, M., Trisunaryanti, W., Falah, I.I., Kartini, I., and Sutarno, 2014, *Int. J. Innovation Appl. Stud.*, 7 (3), 849–856.
4. Liu, J., Li, Z., He, C., Fu, R., Wu, D., and Song, S., 2010, *Int. J. Hydrogen Energy*, 36 (3), 2250–2257.
5. Ting, C.C., Wu, H.Y., Vetrivel, S., Saikia, D., Pan, Y.C., Fey, G.T.K., and Kao, H.M., 2010, *Microporous Mesoporous Mater.*, 128 (1-3), 1–11.
6. Kosuge, K., and Singh, P.S., 2001, *Microporous Mesoporous Mater.*, 44-45, 139–145.
7. Wang, X., Li, W., Zhu, G., Qiu, S., Zhao, D., and Zhong, B., 2004, *Microporous Mesoporous Mater.*, 71 (1-3), 87-97.
8. Coradin, T., Bah, S., and Livage, J., 2004, *Colloids Surf., B*, 35 (1), 53–58.
9. Yang, J., Zhai, Y., Deng, Y., Gu, D., Li, Q., Wu, Q., and Bo. Y.H., 2010, *J. Colloid Interface Sci.*, 342 (2), 579–585.
10. Bele, M., Gaberscek, M., Dominko, R., Drofenik, J., Zupan, K., Komac, P., Kucevar, K., Musevic, I., and Pejovnik, S., 2002, *Carbon*, 40 (7), 1117–1122.
11. Ge, J., Shi, J., and Chen, L., 2009, *Carbon*, 47 (4), 1192–1195.
12. Kang, S., Jian-chun, J., and Dan-dan, C., 2011, *Biomass Bioenergy,* 35 (8), 3643–3647
13. Liou, T.H., 2010, *Chem. Eng. J.,* 158 (2), 129–142.
14. Böhme, K., Einicke, W.D., and Klepel, O., 2005, *Carbon*, 43 (9), 1918–1925.
15. Sobiesiak, M., 2012, *New Carbon Mater.*, 27 (5), 337–343.
16. Guo, R., Guo, J., Yu, F., and Gang, D.D., 2013, *Microporous Mesoporous Mater.*, 175, 141–146.
17. Hayakawa, S., Kanaya, T., Tsuru, K., Shirosaki, Y., Osaka, A., Fujii, E., Kawabata, K., Gasqueres, G., Bonhomme, C., Babonneau, F., Jäger, C., and Kleebe, H.J., 2013, *Acta Biotheor.*, 9 (1), 4856–4867.
18. Diefallah, E.M., 1992, *Thermochim. Acta*, 202, 1–16.
19. Frunza, L., 2003, *Microporous Mesoporous Mater.*, 11 (1), 856–860.
20. Zhu, S., Zhou, H., Hibino, M., Honma, I., and Ichihara, M., 2004, *Mater. Chem. Phys.*, 88 (1), 202–206.